Biol. Cybern. 83, 171–183 (2000)

Biological Cybernetics

How honeybees make grazing landings on flat surfaces

M. V. Srinivasan[1], S. W. Zhang[1], J. S. Chahl[1], E. Barth[2], S. Venkatesh[3]

[1] Centre for Visual Science, Research School of Biological Sciences, Australian National University, P.O. Box 475, Canberra, A.C.T. 2601, Australia
[2] Institute for Signal Processing, Medical University of Lübeck, Ratzeburger Allee 160, 23538 Lübeck, Germany
[3] Department of Computer Science, School of Computing, Curtin University, GPO Box U 1987, Perth, WA 6001, Australia

Received: 21 June 1999 / Accepted in revised form: 20 March 2000

Abstract. Freely flying bees were filmed as they landed on a flat, horizontal surface, to investigate the underlying visuomotor control strategies. The results reveal that (1) landing bees approach the surface at a relatively shallow descent angle; (2) they tend to hold the angular velocity of the image of the surface constant as they approach it; and (3) the instantaneous speed of descent is proportional to the instantaneous forward speed. These characteristics reflect a surprisingly simple and effective strategy for achieving a smooth landing, by which the forward and descent speeds are automatically reduced as the surface is approached and are both close to zero at touchdown. No explicit knowledge of flight speed or height above the ground is necessary. A model of the control scheme is developed and its predictions are verified. It is also shown that, during landing, the bee decelerates continuously and in such a way as to keep the projected time to touchdown *constant* as the surface is approached. The feasibility of this landing strategy is demonstrated by implementation in a robotic gantry equipped with vision.

1 Introduction

Unlike vertebrates, insects have immobile eyes with fixed-focus optics. Therefore, they cannot infer the distances to objects or surfaces from the extent to which the directions of gaze must converge to view the object, or by monitoring the refractive power that is required to bring the image of the object into focus on the retina. Furthermore, compared with human eyes, the eyes of insects are positioned much closer together and possess inferior spatial acuity (Horridge 1977). Therefore, the precision with which insects could estimate range through binocular stereopsis would be much poorer and restricted to relatively small distances, even if they possessed the requisite neural apparatus (Srinivasan 1993). Not surprisingly, then, insects have evolved alternative strategies for dealing with the problems of visually guided flight. Many of these strategies rely on using image motion, generated by the insect's own motion, to infer the distances to obstacles and to control various manoeuvres (Horridge 1987; Srinivasan 1993, 1998).

Visual control of landing is a case in point. The seminal work of Gibson (1950) has highlighted the optic-flow cues that can be brought to bear in controlling the landing of an aircraft. Studies of landing behaviour in flies have revealed that, as a surface is approached, the expansion of the image of the surface provides strong cues that are used to control deceleration and trigger extension of the legs in preparation for contact (Goodman 1960; Eckert and Hamdorf 1980; Wagner 1982; Borst and Bahde 1988). There is also evidence that the rate of expansion of the image is used to infer the time to contact the surface, even if the insect does not possess explicit information about the speed of its flight or the distance to the surface (Wagner 1982).

However, when an insect makes a grazing landing on a flat surface, cues derived from image expansion are relatively weak. This is because the dominant pattern of image motion is then a translatory flow in the front-to-back direction. Given that flying insects often make grazing landings on flat surfaces, what are the processes by which such landings are orchestrated?

Here we investigate experimentally the visuomotor control strategies employed by bees when they make grazing landings on a horizontal surface. We also assess the feasibility of these strategies by implementing them in a computer-controlled gantry equipped with vision.

A preliminary study of landing bees was published in Srinivasan et al. (1996).

2 Experimental methods

A group of six bees were individually marked and trained to collect a reward consisting of a drop of sugar water placed on a horizontal wooden surface consisting of a 1 m × 1 m sheet of particle board. The drop was offered on a piece of transparent acetate paper (5 cm × 5 cm) to prevent contamination of the surface by sugar

Correspondence to: M. V. Srinivasan
(e-mail: M. Srinivasan@anu.edu.au;
Tel.: +61-2-62492409; Fax: +61-2-62493808)

solution or pheromones. During training, the location of the reward was varied randomly every 5 min. This ensured that the bees did not learn to land at a fixed position, say, in relation to external landmarks. After training for half a day, the reward was removed and the flight trajectories of bees landing on the surface were filmed at 25 frames/s by a video camera placed 2.5 m above the surface. In the video films marked bees could be distinguished from unmarked ones, but individual marked bees could not be distinguished from each other reliably because of the relatively large distance of the camera from the surface. Only data from marked bees were used. Our results show analyses of different landing trajectories, some of which are probably from different bees and some from the same bee.

The experiments were conducted outdoors on clear days with the sun at an elevation of approximately 45°. This arrangement allowed the height of the bee to be monitored in terms of the horizontal distance between the bee and its shadow on the surface. Height was calibrated in terms of the length of the shadow cast by a vertical rod of a known height. Figure 1 illustrates the experimental setup. It also shows a typical landing trajectory, where the dark symbols represent positions of the bee in successive video frames and the light symbols corresponding positions of her shadow. As time proceeds, the bee's height above the surface decreases, causing the horizontal distance between the bee and the shadow to decrease. Finally, the images of the bee and her shadow coincide, indicating that she has landed.

This technique, first employed by Zeil (1993), enabled the flight trajectories of the bees to be captured in three dimensions. The technique is accurate, provided the height of the bee is small compared to the height of the camera (in effect, the camera is assumed to be at infinity). Given that the camera was 2.5 m above the surface, and that bees seldom flew at heights greater than 20 cm, the resulting data were sufficiently accurate for our purpose.

Trajectories of landing bees were reconstructed in three dimensions by digitising the positions of the bee and the shadow in the video images, using a computer-assisted digitisation package (Frame grabber: Screen Machine, Munich; Software: Unimark, developed by R. Voss and J. Zeil, Tübingen). The position of the bee in each video frame was registered by a single point, corresponding to the approximate location of the head. A similar procedure was used to register the position of the bee's shadow. The orientation of the body axis was not measured.

Raw data from a video film sequence of a landing are shown in Fig. 2a. The 3-d reconstruction of the trajectory is shown in Fig. 2b. From this data, the time courses of (1) the height above the surface (h; cm), (2) the horizontal (or forward) flight speed (V_f; cm/s), (3) the descent speed (V_d; cm/s), (4) the horizontal distance travelled (cm), and the angular velocity of the motion of the image of the ground in the eye (ω; degrees/s) were computed and their relationships analysed as described in Sect. 3. These variables are illustrated in Fig. 2c. In this and subsequent figures, the orientation of the bee is not shown.

The particle board surface provided a low-contrast texture against which both the bee and her shadow were clearly visible in the video images. When the surface was moved horizontally as the bee approached to land on it, the bee drifted in the direction of motion of the surface (data not shown). It is therefore clear that the surface contained sufficient visual contrast to be detectable by the bees, and that the bee's visual system was capable of sensing the motion of the image of the surface.

Control experiments using a landing surface that carried a high-contrast black-and-white Julesz texture, which rendered the bee's shadow almost invisible, revealed no significant differences in the characteristics of the landing trajectories. Therefore, it is very unlikely that the bee's landings were influenced by the presence of the shadow.

3 Experimental results

Figure 3a shows raw data for a typical landing trajectory. The circles represent successive positions of the bee and the stars the corresponding positions of her shadow. Also shown are the length and direction of the shadow cast by the calibration marker.

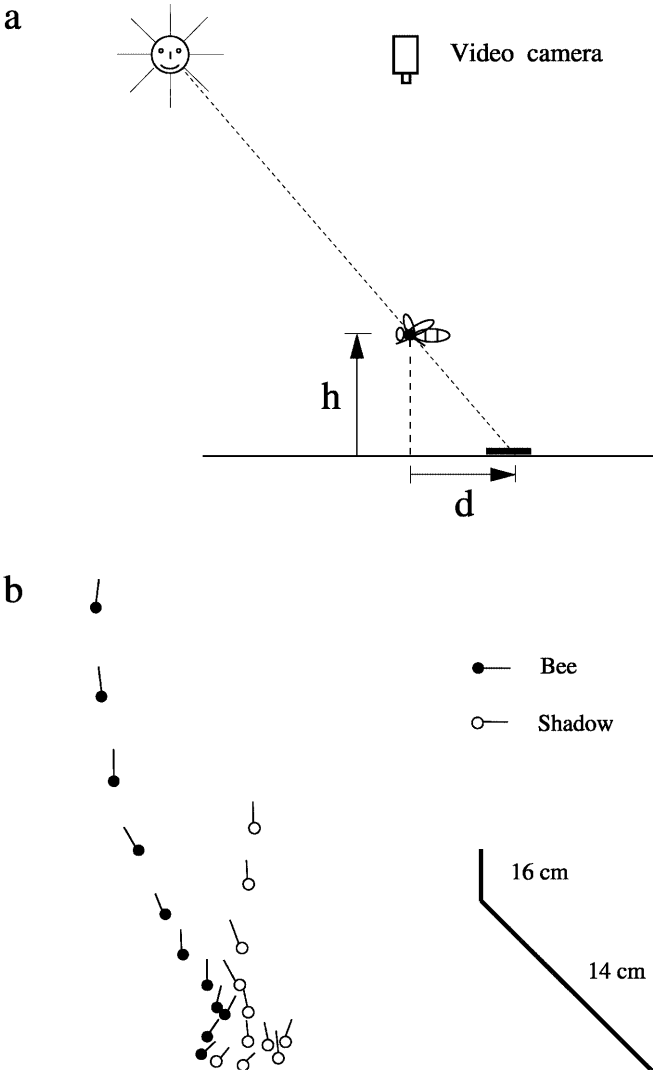

Fig. 1. **a** Experimental arrangement for filming landing trajectories in three dimensions. The horizontal distance d between the bee and her shadow is proportional to her height h above the surface. **b** Example of a landing trajectory, as filmed from above. Positions and orientations of the bee and her shadow are shown every 40 ms. The *dots* represent head positions and the *lines* the body orientations of the bee and her shadow. Also shown are images of the vertical calibration rod and its shadow

Figure 3b–d shows the results of various analyses of the trajectory. A plot of the height of the bee above the surface, against horizontal distance travelled, is shown in Fig. 3b. Horizontal distance travelled is measured as the cumulative length of the flight trajectory as seen in plan, irrespective of whether the trajectory is straight or curved. The angle of final descent was determined from this plot as the slope of the linear regression through the second half of the data points. This measure provided a good estimate of the slope of the curve just prior to touchdown. In this example, the final descent angle is about 52°.

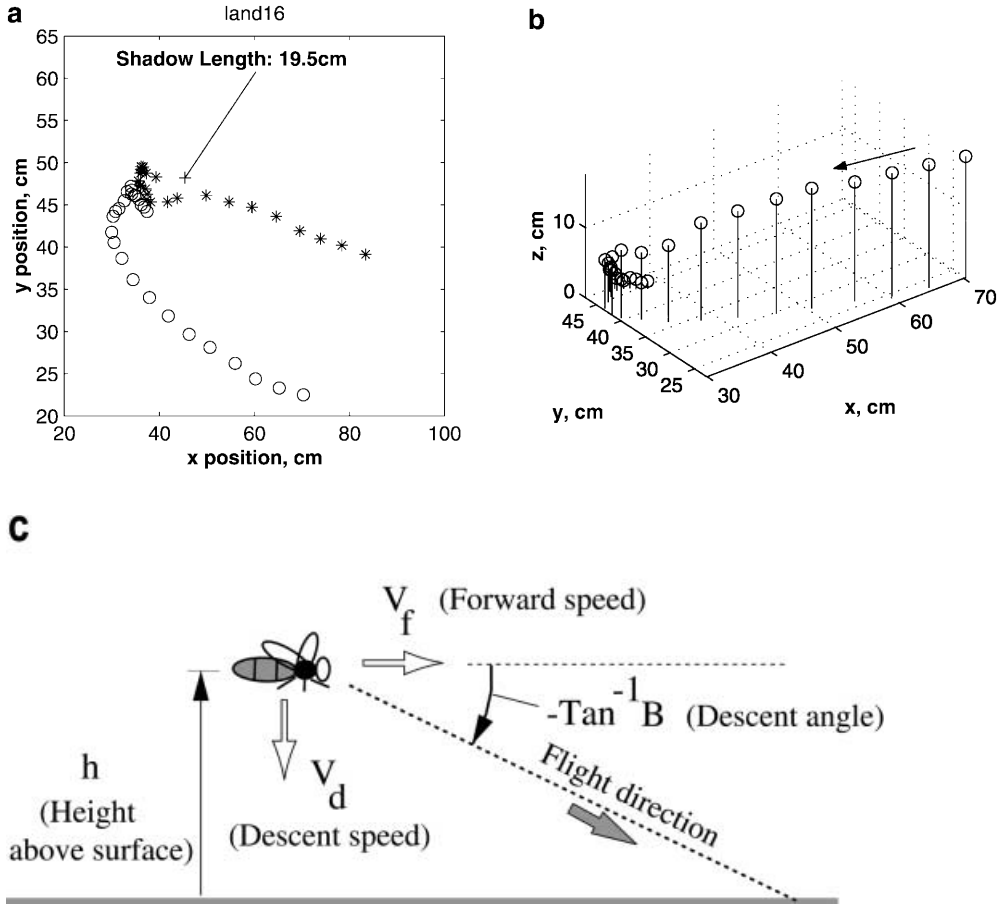

Fig. 2. **a** Raw data from a landing trajectory, showing positions of bee (*circles*) and corresponding positions of the bee's shadow (*stars*) at 40-ms intervals, as viewed from above. The *line* depicts the length and orientation of the shadow cast by the vertical calibration marker. **b** A 3-d view of trajectory, reconstructed from the raw data of **a**. *Vertical lines* depict height above surface. **c** Illustration of some of the variables analysed to investigate the control of landing. h (cm): height above surface; V_f (cm/s): horizontal (forward) flight speed; V_d; (cm/s): vertical (descent) speed; $-\tan^{-1} B$ (deg or rad): descent angle, where B is the ratio of instantaneous descent speed to instantaneous forward speed

Figure 3c shows a plot of the variation of the horizontal speed of the bee with her height above the surface. This data reveals one of the most striking and consistent observations of this study: horizontal speed is roughly proportional to height, as indicated by the linear regression on the data. When a bee flies at a horizontal speed of V_f cm/s at a height of h cm, the angular velocity ω of the image of the surface directly beneath the eye is given by $\omega = \frac{V_f}{h}$ rad/s. From this relationship it is clear that if the bee's horizontal flight speed is proportional to her height above the surface (as in Fig. 3c), then the angular velocity of the image of the surface, as seen by the eye, must be constant as the bee approaches it. This angular velocity is given by the slope of the regression line and corresponds to 8.34 rad/s (478°/s) in this example. The relationship between the image angular velocity (calculated using the above expression) and bee height is plotted in Fig. 3d. We see that the image velocity is roughly constant until the bee is very close to the surface. The dashed line depicts the average image velocity of (478°/s), calculated from the linear regression in Fig. 3c. Just prior to touchdown, when the bee is very close to the surface, the image velocity appears to vary erratically between unusually high and low values. This is to be expected, since, just before touchdown, both flight speed and height are small, so that small variations in either parameter (or small errors in their measurement) can produce relatively large fluctuations in the image velocity, which is computed as the ratio of V_f to h.

Figure 4 shows the variation of flight speed with height above the surface, analysed for four more landing trajectories. In each case the relationship is close to linear, as indicated by the high values of the regression coefficients. The angular velocity of the image varies from one trajectory to another but is maintained at an approximately constant value in any given landing. An analysis of 26 landing trajectories reveals a mean image angular velocity of 500.5 ± 268.4 (SD) degrees/s.

Figure 5 shows the variation of height with horizontal distance travelled, for four landing trajectories. Linear regressions, performed on the data points corresponding to the second half of each trajectory, reveal descent angles ranging from 22° to 41°. The exact value varies between trajectories but is fairly constant for any given trajectory. An analysis of 25 landing trajectories reveals a mean descent angle of $-27.8 \pm 13.8°$ (SD). Thus, in general, the descent angles are quite shallow.

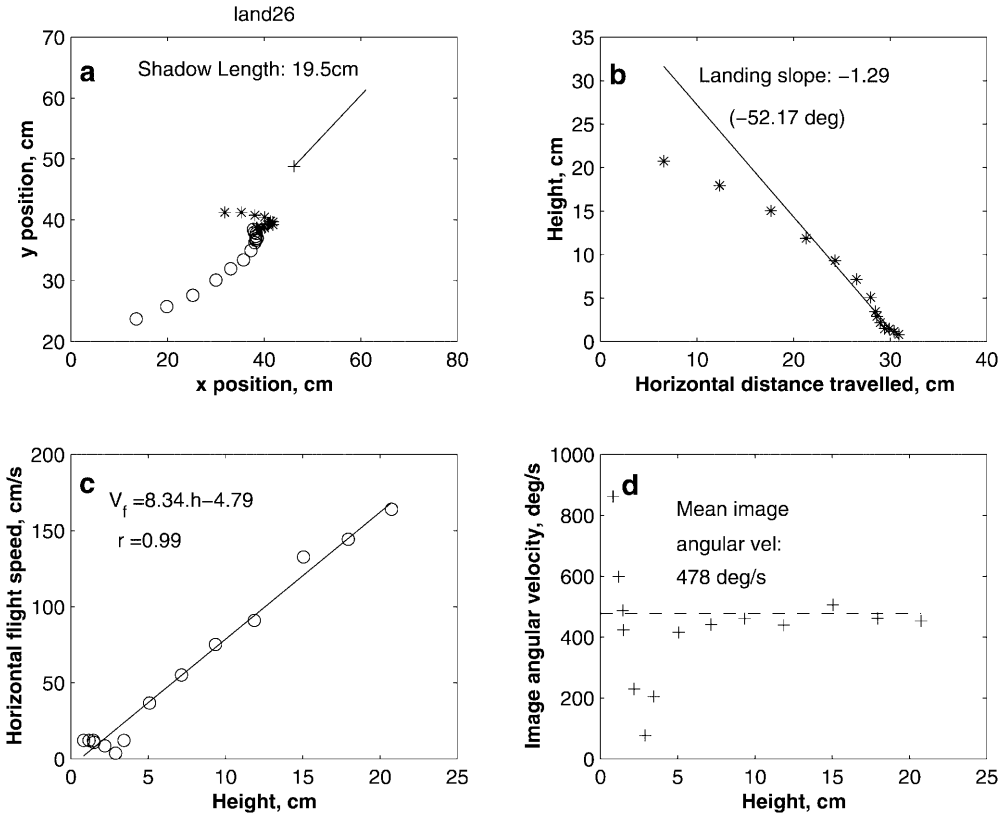

Fig. 3a–d. Analysis of a landing trajectory. **a** Raw data, as in Fig. 2a. **b** Variation of the height of the bee above the surface, as a function of the horizontal distance travelled. The straight line is a linear regression drawn through the second half of the points, to determine the landing slope. **c** Variation of horizontal flight speed (V_f) with height (h) above the surface. The *straight line* is a linear regression through the points, as represented by the equation. The regression coefficient is denoted by r. **d** Variation of calculated image angular velocity with bee height. The *dashed line* represents the mean angular velocity of the image, calculated from the slope of the regression line in **c**

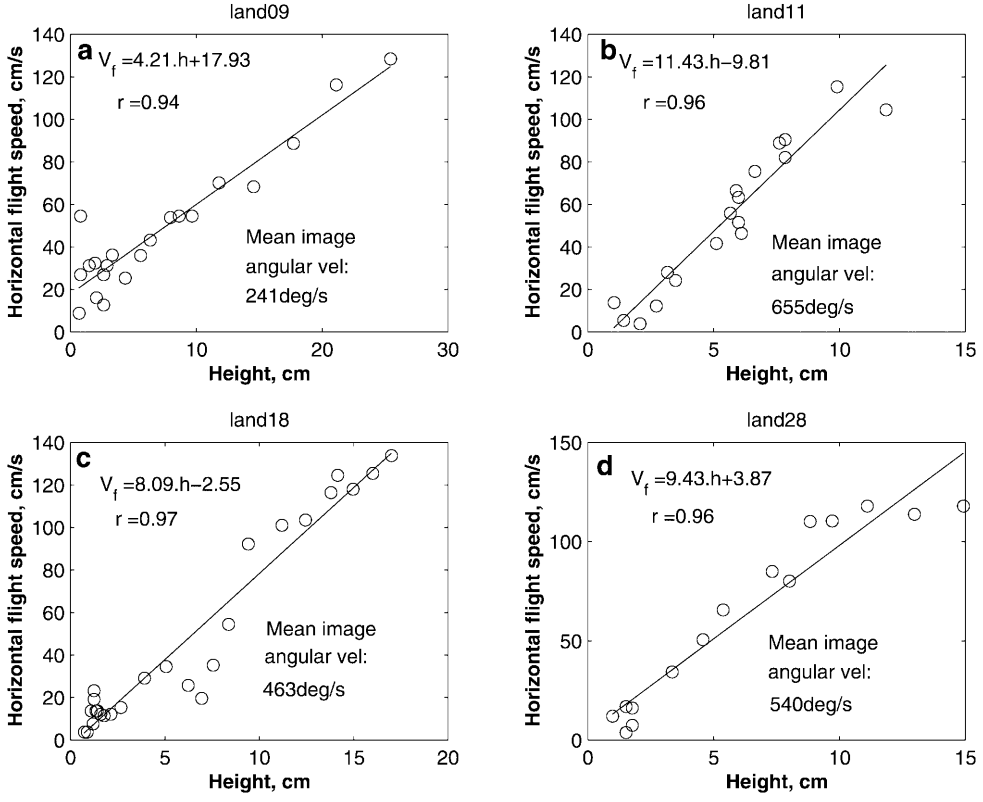

Fig. 4a–d. Variation of horizontal flight speed (V_f) with height (h) above the surface, for four different landing trajectories. The *straight lines* are linear regressions through the data, as in Fig. 3c

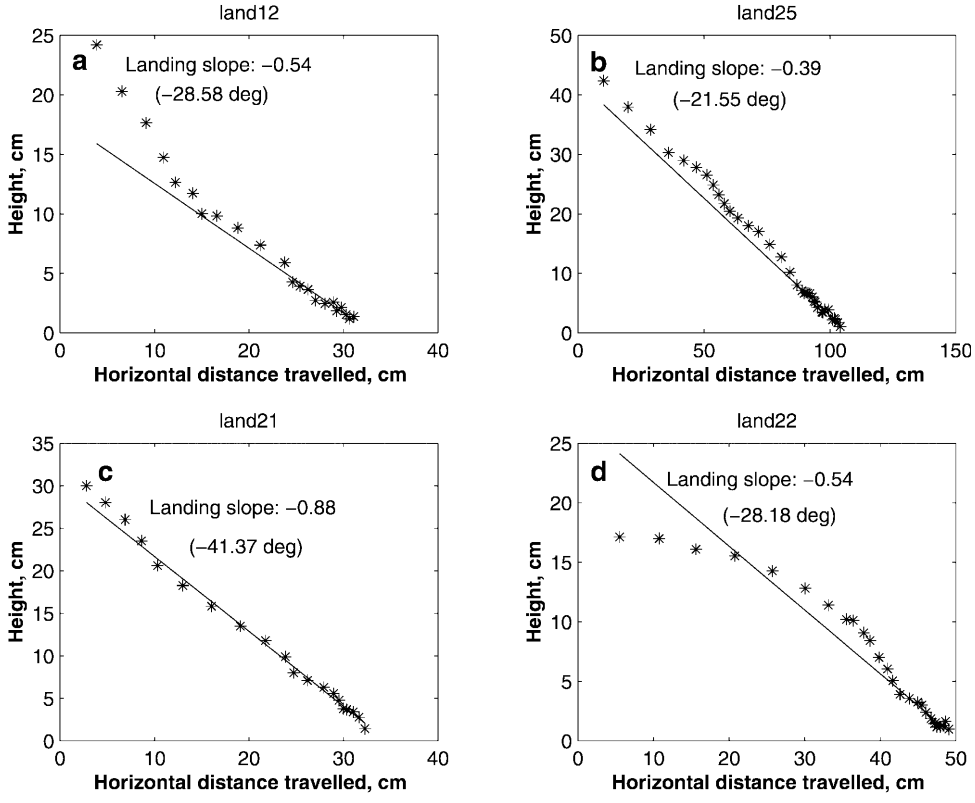

Fig. 5a–d. Variation of bee height as a function of the horizontal distance travelled, for four different landing trajectories. The *straight lines* are linear regressions drawn through the second half of the points, to determine the landing slope

The results shown in Figs. 3–5 reveal two important characteristics. First, bees landing on a horizontal surface tend to approach the surface at a relatively shallow descent angle. Second, landing bees tend to hold the angular velocity of the image of the ground constant as they approach it.

What is the significance of holding the angular velocity of the image of the ground constant during landing? One important consequence is that the horizontal speed of flight is then automatically reduced as the height decreases. In fact, by holding the image velocity constant, the horizontal speed is regulated to be proportional to the height above the ground, so that when the bee finally touches down (at zero height), her horizontal speed is zero, thus ensuring a smooth landing. The attractive feature of this simple strategy is that it does not require explicit measurement or knowledge of the speed of flight, or the height above the ground. Thus, stereoscopic methods of measuring the distance of the surface (which many insects probably do not possess) are not required. What is required, however, is that the insect be constantly in motion, because the image motion resulting from the insect's own motion is crucial in controlling the landing.

4 A model of the landing process

Based on the above experimental findings, we attempt in this section to develop and test a model of the landing process. The model is developed with reference to Fig. 2c.

Ideally, the landing strategy should ensure that the speed of flight in the horizontal (forward) direction as well as the downward direction (descent speed) are reduced as the ground is approached. We have already seen from the experimental results that the speed of forward flight is controlled by holding the angular velocity of the image of the ground constant. As shown above, this ensures that the instantaneous forward flight speed, $V_f(t)$, is proportional to the instantaneous height $h(t)$ above the ground. That is,

$$V_f(t) = \omega h(t) \tag{1}$$

where the constant of proportionality, ω, is the angular velocity of the image in radians per second.

A safe landing requires that the speed of flight in the *downward* direction (descent speed) is also reduced as the ground is approached. This can be achieved by making the instantaneous downward speed, $V_d(t)$, proportional to the instantaneous forward speed. That is,

$$V_d(t) = -\frac{dh(t)}{dt} = BV_f(t) \tag{2}$$

where B is a constant of proportionality corresponding to the ratio of V_d to V_f.

In other words, a plot of height versus horizontal distance travelled should be a straight line with a (negative) slope of B. Such a linear relationship is indeed exhibited by the experimental data, as can be seen from the plots of Figs. 3b and 5. This in turn implies that landing bees not only control their forward flight speed according to the relationship specified by (1) but

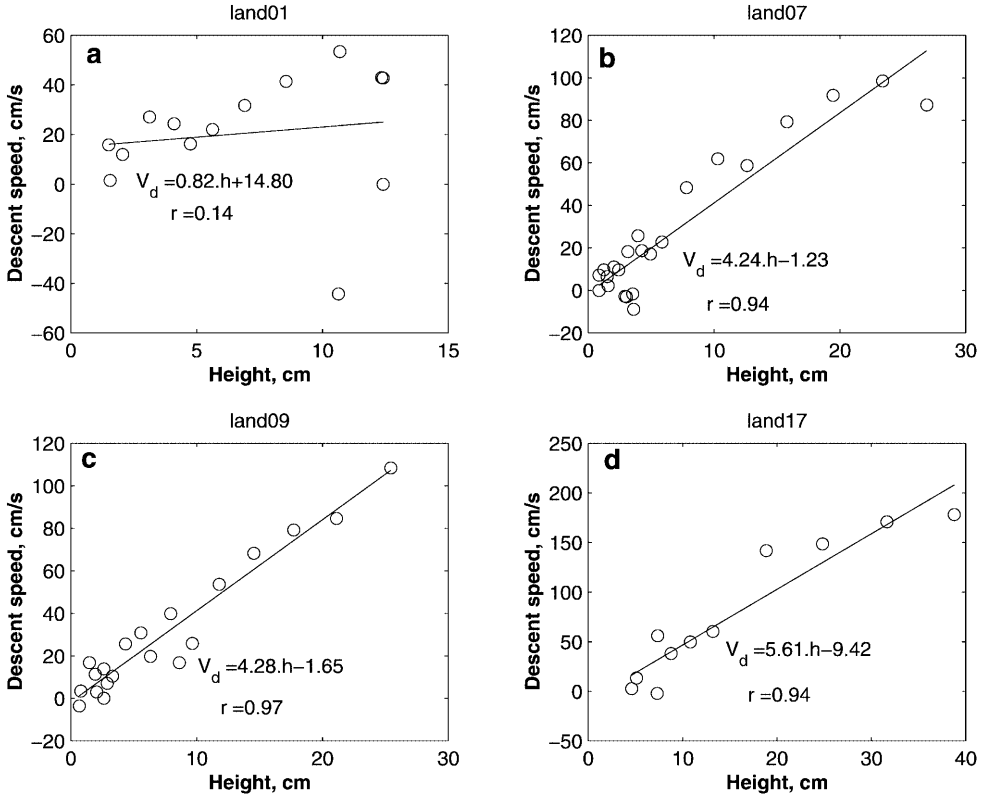

Fig. 6a–d. Variation of descent speed (V_d) with height (h) above the surface, for four different landing trajectories. The *straight lines* are linear regressions through the data, as in Figs. 3c and 4

also make the rate of descent proportional to the forward flight speed by linking the two speeds together as specified by (2). This control strategy ensures that when the bee finally touches down, she is moving with zero speed in the forward as well as the downward directions. In other words, the touchdown is perfectly smooth.

One consequence of such a landing strategy, in which the speed of descent is linked to the forward speed, would be that the descent speed, like the forward speed, is proportional to the height above the ground. Plots of descent speed versus height are shown for four examples in Fig. 6. In most cases, there is a strong correlation between descent speed and height. However, this correlation is not as consistent as that between forward speed and height. We suspect that the reason is that forward speed is controlled by image velocity in a direct, reflexive way, whereas descent speed is in turn linked to forward speed in a less rigid, "voluntary" way that depends partly on whether or not the bee is in "landing mode". For example, in Fig. 6a, most of the points lie close to a straight line except those corresponding to large heights. Inspection of the actual landing trajectory reveals that in the beginning of the trajectory the bee was actually climbing or flying level: it was not in the landing mode. Thus, even in instances where a bee does not actually land on the surface but simply cruises over it, we find that forward speed is tightly coupled to height, whereas vertical speed is not. An example of a cruising flight is illustrated in Fig. 7. Here the bee alternately decreases and increases her altitude above the surface, without actually landing on it (Fig. 7b). Figure 7c shows that, even in this situation, the instantaneous forward flight speed is adjusted to be roughly proportional to the instantaneous height above the surface. In other words, even during cruising, the image velocity of the ground is held approximately constant, irrespective of the height above the surface (Fig. 7d). But the speed of descent is not correlated with the forward speed, because the bee is not in landing mode. The descent speed can be positive, negative, or zero depending upon whether the cruising bee chooses to descend, climb, or fly level.

Let us now consider further predictions of the proposed model for landing.

Substituting (1) into (2), we obtain

$$B\omega h(t) + \frac{\mathrm{d}h(t)}{\mathrm{d}t} = 0 \tag{3}$$

This differential equation can be solved for $h(t)$ to yield

$$h(t) = h(t_0)\mathrm{e}^{-\omega B(t-t_0)} \tag{4}$$

where $h(t_0)$ is the height at the initial time $t = t_0$.

Equation (4) therefore predicts that, during landing, the height should decrease exponentially with time. The four examples shown in Fig. 8 reveal that the variation of height with time does indeed approximate an exponential function very closely, thus reinforcing the model's validity.

The exponential decay of height with time [Eq. (4)] implies, of course, that touchdown ($h = 0$) would occur only at infinite time. This, however, is not a problem in reality because extension of the legs prior to landing

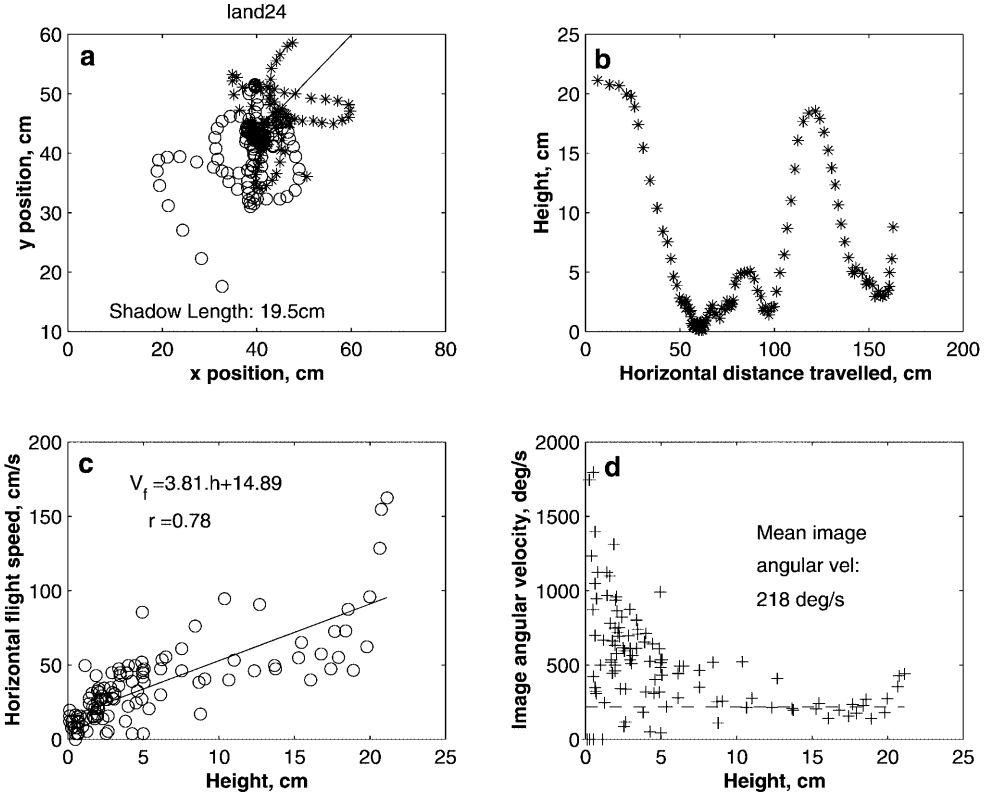

Fig. 7a–d. Analysis of a "cruising" trajectory in which the bee did not land. Details as in Fig. 3

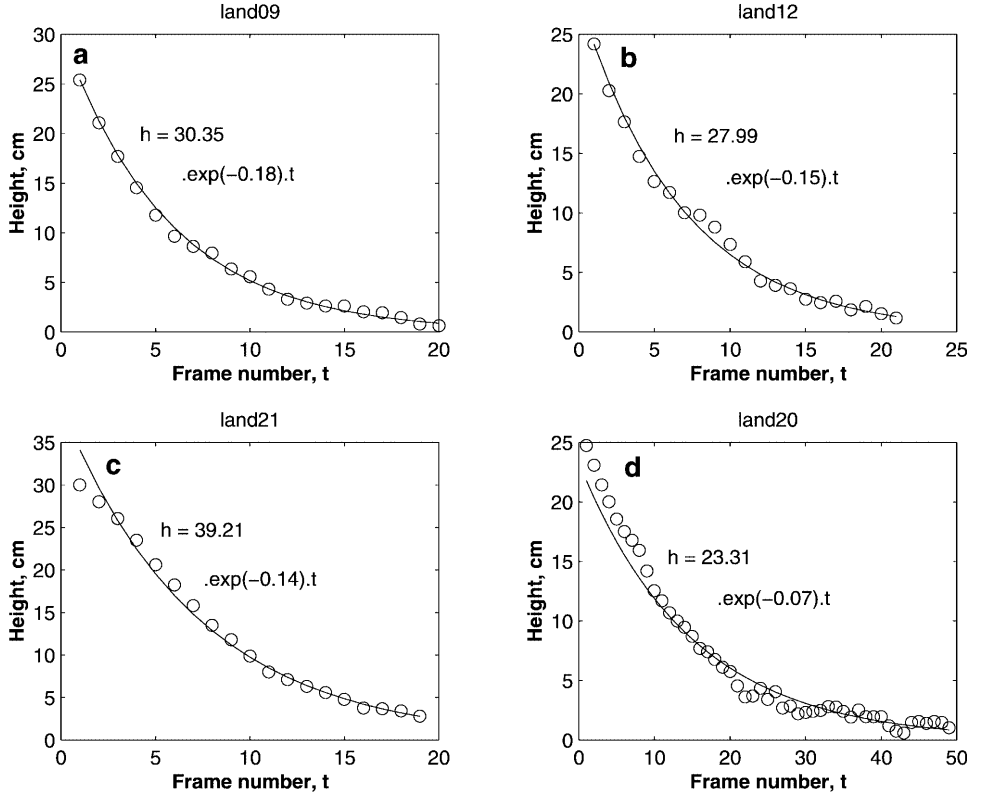

Fig. 8a–d. Variation of height (h) with time (t, denoting frame number) for four different landing trajectories. The interframe interval is 40 ms. The curves show least-squares fits of exponential functions as specified by (4)

ensures that touchdown usually occurs at a nonzero height above the ground. The time taken to arrive within any given, nonzero distance from the ground is, of course, finite. For example, if the touchdown height is h_{touch}, the time T taken to descend to this height from an initial height $h(t_0)$ can be calculated from (4) as

$$T = \frac{1}{\omega B}\log\left[\frac{h(t_0)}{h_{\text{touch}}}\right] \tag{5}$$

The model also predicts the way in which the forward and downward components of flight speed should evolve during landing. Inserting (4) into (1), we obtain

$$V_{\text{f}}(t) = \omega h(t_0)\mathrm{e}^{-\omega B(t-t_0)} \tag{6}$$

This implies that the forward flight speed should decrease exponentially with time. Inserting (6) into (2), we obtain

$$V_{\text{d}}(t) = B\omega h(t_0)\mathrm{e}^{-\omega B(t-t_0)} \tag{7}$$

This implies that the downward speed (speed of descent) should also decrease exponentially with time.

Our data reveal that the forward and descent speeds indeed decrease approximately exponentially with time. We have not shown the plots here, but these predictions should obviously hold because if height decreases exponentially with time (as demonstrated by the data in Fig. 8), it follows that the forward and descent speeds should also decrease exponentially with time, as predicted by (6) and (7). The reason is that height, forward speed, and descent speed are linearly related to each other.

Yet another prediction of the model has to do with the way in which the cumulative horizontal distance travelled by the bee increases with time. This distance, H, is obtained by integrating over time the expression for the forward flight speed, $V_{\text{f}}(t)$, from (6):

$$H = \int_{t_0}^{t} V_{\text{f}}(t)\mathrm{d}t = \int_{t_0}^{t} \omega h(t_0)\mathrm{e}^{-\omega B(t-t_0)}\ \mathrm{d}t \tag{8}$$

Integration yields

$$H = \frac{h(t_0)}{B}\left[1 - \mathrm{e}^{-\omega B(t-t_0)}\right] \tag{9}$$

Equation (9) predicts that the cumulative horizontal distance travelled should increase as a saturating exponential function of time. The four examples shown in Fig. 9 reveal that the variation of horizontal distance travelled with time does indeed approximate a saturating exponential function very closely. This finding further reinforces the model's validity.

To summarise the results, we find that bees regulate the forward speed of their flight by holding constant the velocity of the image of the ground in the eye. As a consequence, the forward speed is tightly linked to the height above the ground and is proportional to it. Furthermore, when a bee is in "landing mode", the rate of descent is coupled to the forward speed and is proportional to it. The coupling factor B determines the angle of descent. This landing strategy ensures that both the forward speed and the descent speed are reduced progressively as the bee approaches the ground and are both zero at touchdown. Such a model predicts that, during landing, the height above the ground should decrease exponentially with time. It also predicts that the cumulative horizontal distance travelled should increase

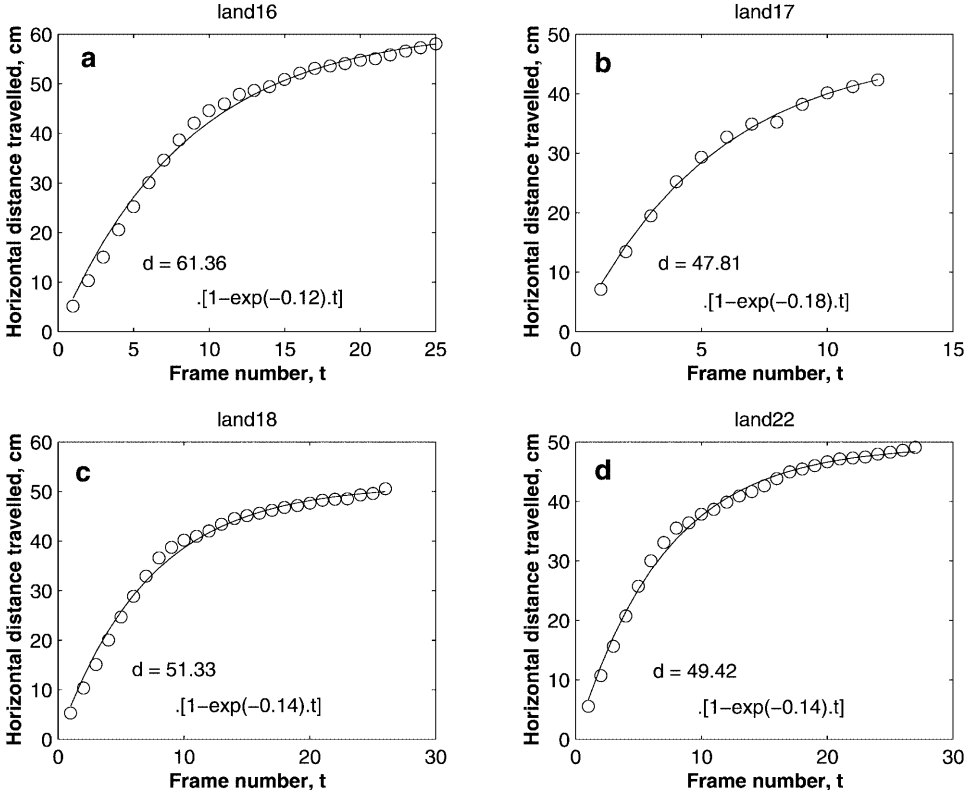

Fig. 9a–d. Variation of cumulative horizontal distance travelled (H) with time (t, denoting frame number) for four different landing trajectories. The interframe interval is 40 ms. The curves show least-squares fits of saturating exponential functions as specified by (9)

as a saturating exponential function. We have been able to verify both of these predictions experimentally.

5 Feasibility of the honeybee's landing strategy

We have tested the feasibility of the landing strategy described above by implementing it in a computer-controlled gantry robot carrying a visual system. Vision is provided by a video camera mounted on the gantry head, which can be translated in three dimensions (x, y, and z) and rotated about one axis (z). The head can traverse a volume of space measuring 2.5 m long (x), 2 m wide (y), and 1 m high (z). For the purpose of implementing the landing strategy, translatory motion of the camera is restricted to the forward (x) and downward ($-z$) directions. There is no rotary motion about the z axis.

The system is placed under closed-loop control by using a computer to analyse the motion in the image sequence captured by the camera and to control the motion of the gantry. A view of the gantry and camera is shown in Fig. 10.

The camera, facing downwards and viewing the ground, has a visual field of 52° in the x direction and 70° in the y direction. The image of the ground is captured by an array of 768 × 576 pixels. The velocity of image motion is measured by using an image interpolation algorithm developed in our laboratory. Details of the algorithm are given in Srinivasan (1994). Prior to measuring motion, the image is spatially low-pass filtered by a Gaussian function of width (standard deviation) 0.1°. The reference images that are required by the image interpolation technique for computing image motion (see Srinivasan 1994) are separated by 0.5°. Image motion is computed within windows centred on each image pixel. The window is defined by a Gaussian weighting function of width (standard deviation) 1°. The global image velocity, obtained by averaging velocity measurements over all pixels, is used to control the motion of the gantry. The floor, defined to be the landing surface, is covered with a visual texture consisting of a black-and-white Julesz pattern of pixel size 1 cm square.

Fig. 10. View of robotic gantry, showing camera head and visual texture on the floor

Landing is controlled as follows. The system is required to maintain a constant descent angle ($\tan^{-1} B$) and a constant image angular velocity, ω_{set}, as it descends. In the first time step, the gantry moves the camera head along the direction of descent at an arbitrarily chosen initial speed. The image velocity is measured during this step, using the image interpolation algorithm. Let us denote the measured image velocity by ω_{meas}. In the next step, the speed of motion of the head is increased or decreased, depending upon whether the measured image velocity is lower or greater than the set image velocity. Specifically, the forward speed $V_{\text{f}}(i+1)$ of the camera during the next step is related to the current speed $V_{\text{f}}(i)$ by

$$V_{\text{f}}(i+1) = V_{\text{f}}(i)\,\frac{\omega_{\text{set}}}{\omega_{\text{meas}}} \tag{10}$$

The speed of descent is also corrected by the same factor, since the forward and descent speeds are proportional to each other and linked by the desired angle of descent. This speed correction ensures that the image velocity during the next step will have the desired value ω_{set}, provided the camera maintains its present altitude. However, since the camera continues to descend during the new step, the forward speed in the following step would have to be reduced further. Thus, both the forward and descent speeds decrease continuously as the camera descends, reaching very low values when the camera is close to the ground.

Landing trajectories generated by the gantry using this procedure are shown in Fig. 11a for three different descent angles: −26.5°, −45°, and −63.5°. The image velocities maintained during these three landings are shown in Fig. 11b. It is clear that the image velocity, though somewhat noisy, is held reasonably constant. The height of the camera decreases exponentially with time (Fig. 11c), as do the forward speed and the speed of descent. These behaviours are as expected from the proposed control strategy. Comparable results were obtained when the floor was covered with other textures, such as a newspaper, or with twigs, bark, and leaves to simulate a more natural outdoor environment (data not shown).

The results with the robotic gantry therefore suggest that the strategy proposed is a feasible one for landing on flat surfaces. In undulating terrain, the system reduces the forward and descent speeds when the ground

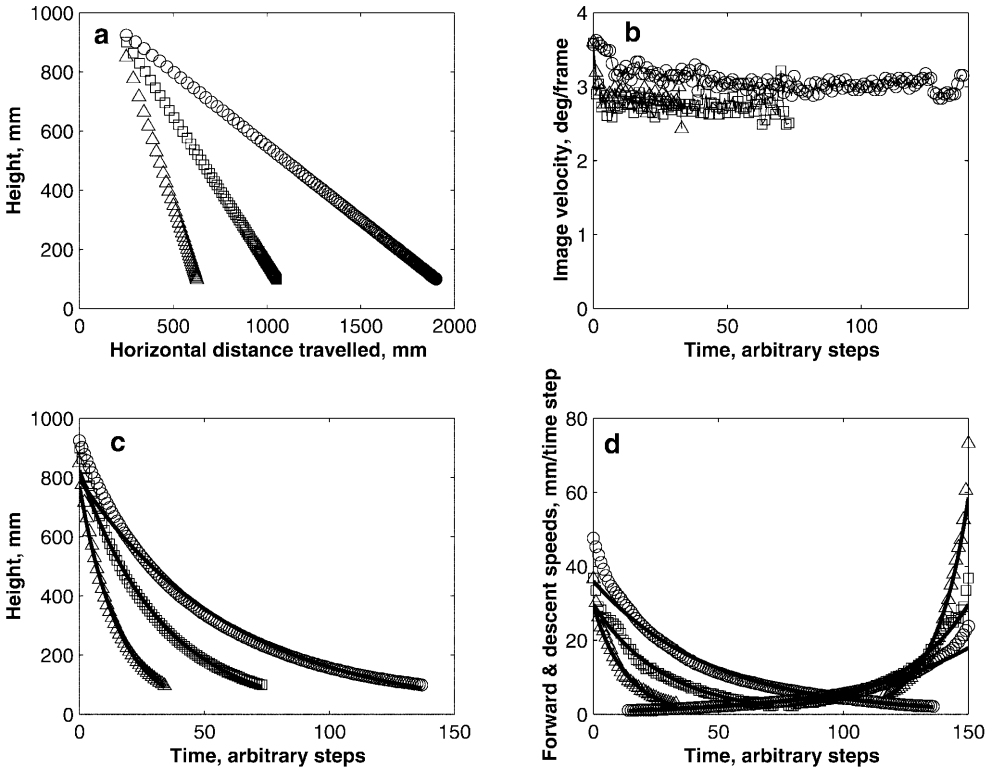

Fig. 11a–d. Landing trajectories generated by the robotic gantry. **a** Height versus distance travelled for three different descent angles: −26.5° (*circles*), −45° (*squares*), and −63.5° (*triangles*). **b** Variation of image angular velocity as a function of time. The symbols in this and other panels refer to the three different descent angles, as in **a**. **c** Variation of height with time. **d** Variation of forward speed and descent speed with time. For clarity the descent speed data are shown on a reversed time scale, decaying from right to left. The *line curves* in **c** and **d** depict least-squares fits of exponential functions to the data

rises towards the camera and increases them when the ground falls away. This is obviously a desirable feature, but it has limitations in that the system cannot cope with a situation in which the ground in front rises abruptly to a level above the camera's current height.

6 Discussion

Our experimental results reveal what appears to be a surprisingly simple and effective strategy for making grazing landings on flat surfaces. A safe, smooth landing is ensured by (1) adjusting the speed of forward flight to hold constant the angular velocity of the image of the surface as seen by the eye, and (2) making the speed of descent proportional to the forward speed. This strategy produces landing trajectories in which the forward speed as well as the descent speed decrease progressively as the surface is approached and are both close to zero at touchdown.

The tendency exhibited by bees to adjust their forward speed according to the speed of the image in the eye is probably not restricted to landing conditions. We have reported earlier that bees flying along a tunnel tend to slow down at narrow sections of the tunnel and speed up at wider sections (Srinivasan et al. 1996). David (1982) found similar behaviour in the vinegar fly *Drosophila*. Our analysis of "cruising" bees (e.g., Fig. 7) also fits this picture. The use of image speed to control forward flight speed therefore appears to be a general, more or less "hard-wired" feature of insect flight.

During landing, however, an additional control mechanism seems to switch on. A vertically downward component of motion is added, the magnitude of which is set to be proportional to the instantaneous forward speed. Presumably, the forward and downward speeds are controlled by the thrust and lift components, respectively, of the average force vector generated by the wings. [In flying *Drosophila*, there is good evidence that lift and thrust co-vary (Goetz and Wandel 1984)]. With such a control strategy in place, all that is needed is to adjust the forward speed (and therefore also the descent speed) so as to maintain a constant image velocity in the eye. This automatically ensures a smooth touchdown, without the need for explicit knowledge about the actual speed of flight or height above the ground at any time. The successful implementation of this strategy in the robotic gantry suggests that this is a feasible mechanism for achieving a safe landing.

Any behaviour that involves making a safe contact with a stationary object – be it landing on a surface or grasping a branch – requires precise sensorimotor control of many of the components that constitute the behaviour. Flies approaching to land on a small object, for example, decelerate sharply at a fixed time before the projected time to contact (Wagner 1982), and gannets plunging into water to catch fish seem to use information on the projected time to contact to decide when to tuck in their wings prior to touching the water surface (Lee and Reddish 1981). Indeed, there is evidence in the literature that many such manoeuvres are controlled by the "time to contact" computed by the visual system through analysis of the optic flow that results from approaching the object or surface (Lee 1976; Lee and Reddish 1981).

Is there any relationship between the landing scheme investigated here and such "time-to-contact" strategies? Consider our bee making a grazing landing on the horizontal surface. If the bee were to approach the surface at a constant speed, then the projected time to touchdown would, of course, decrease linearly with time. In our landing scheme, however, the bee is decelerating continuously. How does the projected time to touchdown evolve under these conditions?

To examine this, we note that the instantaneous forward speed, $V_f(t)$, is related to the height above the surface, h, and the angular velocity ω of the image in the eye as described by (1). We also know that the instantaneous descent speed, $V_d(t)$, is proportional to the forward speed, as specified by (2). The constant of proportionality, B, controls the descent angle. Combining (1) and (2), we obtain $V_d(t) = B\omega h(t)$. Thus, the instantaneous descent speed is proportional to the height $h(t)$ above the surface, the angular velocity ω of the image, and the parameter B. If the bee were to continue to approach the surface at the same flight speed, the projected (anticipated) time to touchdown would be obtained by dividing the current height above the surface by the instantaneous descent speed. Dividing $h(t)$ by the above expression for $V_d(t)$, we see that the projected time to touchdown is given by

$$\text{Projected time to touchdown} = \frac{1}{B\omega}\ \text{s} \qquad (11)$$

Since B is constant, and the image velocity ω is held constant by the landing strategy, it follows that the *projected time to touchdown is constant throughout the landing process*. Thus, the projected time to touchdown does not decrease linearly with time, as it would if the bee approached the surface at constant speed. Neither does the bee decelerate abruptly when the projected time to touchdown falls below a critical value, as flies seem to do before landing on a small target (Wagner 1982). Rather, the landing bee decelerates *continuously*, and in such a way as to maintain a *constant* projected time to touchdown. This, in effect, is the reason why touchdown theoretically requires infinite time. We have already seen in Sect. 3 that landing bees descend at an average angle of about $-28°$ [$B = \tan(28°) = 0.53$] and hold the image velocity in the eye constant at an average value of about $500°$/s ($\omega = 8.73$ rad/s). Inserting these values into (11), we calculate that the average landing bee maintains a constant, projected time to touchdown of about 0.22 s. Thus, it appears that landing bees allow themselves a "safety margin" of a fifth of a second to prepare for touchdown if they were to abandon the prescribed landing strategy at any point, for whatever reason, and proceed toward the ground in the same direction without further deceleration.

Pigeons landing on a perch (Lee et al. 1993) or hummingbirds flying toward a feeder (Lee et al. 1991) appear to employ a somewhat different strategy. There, the animal seems to control its approach by keeping constant the *rate of change* of the projected time to contact. This produces target distance-versus-time functions that take the form $d = (1 - kt)^{\frac{1}{k}}$, where d denotes the normalised distance to the target, t the normalised time, and k the rate of change of the projected time to contact (Lee et al. 1993). The strategy employed by bees landing on a horizontal surface seems to be different: they maintain a *constant* time to contact, implying that the rate of change of this parameter is zero. This strategy generates distance-versus-time functions that decay exponentially [see (4)]. Indeed, it can be shown that the above expression for d tends to the exponential decay function e^{-t} as k tends to zero. Landing pigeons (Lee et al. 1993) and docking hummingbirds (Lee et al. 1991) maintain the rate of change of the projected time to contact at a value of about 0.7. This strategy produces landings that commence with weak braking and finish with strong deceleration. In contrast, the bee's landing strategy, which maintains a constant projected time to touchdown, produces braking that is strongly initially and decays exponentially with time. (The fact that the height decreases exponentially with time, as shown in Fig. 8, implies that higher temporal derivatives of height, such as descent velocity and descent deceleration, also decay exponentially with time.)

It should be noted that the honeybee's landing strategy, though ensuring a smooth touchdown, does not carry any information about when the touchdown will actually occur. How, then, does the bee know when to extend her legs in preparation for this event? One possibility is that the legs are extended when the flight thrust (which should be a reliable indicator of flight speed) has dropped below a critical value, indicating that touchdown is imminent. Additionally, the bee may be able to detect proximity to the ground by sensing changes in her aerodynamic microenvironment. Assuming that the landing bee maintains an average image angular velocity of 500 degrees/s ($\omega = 8.73$ rad/s) and an average descent angle of $-28°$, and that the legs touch the ground when the eye is 5 mm above the surface, we calculate from (1) that the average forward speed at touchdown would be about 4.4 cm/s, and from (2) that the average descent speed at touchdown would be about 2.3 cm/s. Given the relatively low mass of a bee (100 ± 20 mg, R. Maleszka, personal communication), these speeds would seem to be low enough for the legs to absorb the impact of landing without suffering damage.

What are the advantages, if any, of using the strategy that we have described here to control grazing landings? We can think of two attractive features. First, the control of forward and descent speeds is achieved by holding the image velocity ω *constant*. This is potentially useful because it would be desirable to maintain the image velocity at a level at which the visual system is most sensitive to deviations from the "set" velocity, thereby ensuring that the control of flight is as precise as possible. An alternative strategy, for instance, might be to approach the surface at constant speed, decelerating only towards the end. A constant-speed approach, however, would cause the image velocity to increase rapidly as the surface is approached and to reach levels at which the image velocity measurements may no

longer be precise enough for adequate flight control. This situation would be avoided by the bee's strategy, which holds the image velocity constant. A second advantage of holding the image velocity constant would be the by-product of maintaining a constant projected time-to-contact throughout the landing process, as discussed above.

It would be of interest to explore the applicability of the strategy described in this article to guide landing of autonomously flying machines. One approach would be to start by specifying, for example, the maximum safe descent speed, V_{dtouch}, at touchdown. Then, given a prescribed descent angle, (in effect, the parameter B), the forward speed at touchdown, V_{ftouch}, can be calculated as

$$V_{\mathrm{ftouch}} = \frac{V_{\mathrm{dtouch}}}{B} \tag{12}$$

If we assume that touchdown occurs at a height h_{touch} above the surface (where h_{touch} represents the height of the landing gear, for example), then the angular velocity ω_{touch} of the image on the eye at touchdown will be

$$\omega_{\mathrm{touch}} = \frac{V_{\mathrm{ftouch}}}{h_{\mathrm{touch}}}\,\mathrm{rad/s} \tag{13}$$

The control strategy for landing would then simply involve holding the image angular velocity at its critical values, ω_{touch}, throughout the descent. At touchdown, the descent and forward speeds will then be at their specified values.

At what altitude should such a process of landing be initiated? It would be sensible not to commence it when high above the ground, because the exponential decay of height with time would mean that touchdown would take a long time. At a high altitude the image velocity of the ground is likely to be rather low – much lower than the critical value ω_{touch}. Therefore, when one is certain that the machine is at a high altitude (as indicated, for example, by an altimeter), a time-efficient landing strategy would be to lower altitude as rapidly as possible until the image velocity has increased to the critical value. The landing process would then be initiated to bring the machine to a safe touchdown by holding the image velocity constant at ω_{touch}.

Our study has only investigated grazing landings on a flat, horizontal plane. Under these conditions, it is sufficient to control the landing process by monitoring image speed directly beneath the insect (or machine). Although we find that bees make shallow landings on horizontal surfaces, the landing strategy that we have proposed here does not necessarily require that the descent angle be small. In principle, the control strategy should work satisfactorily regardless of the descent angle as long as the angular velocity of the image, as measured in the ventral field of view (i.e. looking directly down at the surface) is held constant. Of course, a problem arises when the surface is approached perpendicularly, because the image velocity in the direction of motion would then be zero, as it corresponds to a pole of the flow field. However, this difficulty could be eliminated by measuring the average image velocity over a larger visual field. In fact, it is not possible to decide from our data whether landing bees measure image velocity only within a narrow field of view in the ventral direction – as we have implicity assumed in our model – or whether they use information such as average image velocity or peak image velocity, obtained by analysing optic flow over a larger visual field. All of these variants of the model would generate similar landing trajectories in which the distance from the surface decreases exponentially with time. Further work is needed to distinguish between these possibilities.

The landing strategy proposed here is valid only for surfaces that are planar, or approximately so. Further work is required to ascertain whether, and how, the control of landing is altered when approaching uneven surfaces. It would then be necessary to look forwards as well as downwards, to avoid cliffs or other obstacles and to modify the present scheme to include ascents where necessary. One can also examine whether simple modifications of the strategy described here can be applied to problems of obstacle avoidance and terrain following [see, for example, Mura and Franceschini (1994)].

Acknowledgements. We thank the referees for their helpful comments. This research was supported partly by a grant from the Australian Defence Science and Technology Organisation, Salisbury, Grant RG 84/97 from the Human Frontiers in Science Program, and Grant N00014-99-1-0506 from the U.S. Defence Advanced Research Projects Agency and the Office of Naval Research. Some of the initial simulations of the model were carried out when E.B., M.V.S., and S.V. were Fellows of the Institute of Advanced Study in Berlin in 1997.

References

Borst A, Bahde S (1998) Visual information processing in the fly's landing system. J Comp Physiol [A] 163: 167–173

David CT (1982) Compensation for height in the control of groundspeed by *Drosophila* in a new, "Barber's Pole" wind tunnel. J Comp Physiol 147: 485–493

Eckert H, Hamdorf K (1980) Excitatory and inhibitory response components in the landing response of the blowfly, *Calliphora erythrocephala*. J Comp Physiol A 138: 253–264

Gibson JJ (1950) The perception of the visual world. Houghton Mifflin, Boston

Goetz KG, Wandel U (1984) Optomotor control of the force of flight in *Drosophila* and *Musca*. II. Covariance of lift and thrust in still air. Biol Cybern 51: 135–139

Goodman LJ (1960) The landing responses of insects. I. The landing response of the fly, *Lucilia sericata*, and other calliphoridae. J Exp Biol 37: 854–878

Horridge GA (1977) Insects which turn and look. Endeavour NS 1: 7–17

Horridge GA (1987) The evolution of visual processing and the construction of seeing systems. Proc R Soc Lond B 230: 279–292

Lee DN (1976) A theory of visual control based on information about time-to-collision. Perception 5: 437–459

Lee DN, Reddish PE (1981) Plummeting gannets: a paradigm of ecological optics. Nature 293: 293–294

Lee DN, Reddish PE, Rand DT (1991) Aerial docking by hummingbirds. Naturwissenschaften 78: 526–527

Lee DN, Davies MNO, Green PR, Van der Weel FR (1993) Visual control of velocity of approach by pigeons when landing. J Exp Biol 180: 85–104

Mura F, Franceschini N (1994) Visual control of altitude and speed in a flying agent. In: Cliff D, Husbands P, Meyer J-A, Wilson SW (eds) From animals to animats III. MIT. Press, Cambridge, Mass., pp 91–99

Srinivasan MV (1993) How insects infer range from visual motion. In: Miles FA, Wallman J (eds) Visual motion and its role in the stabilization of gaze. Elsevier, Amsterdam, pp 139–156

Srinivasan MV (1994) An image-interpolation technique for the computation of optic flow and egomotion. Biol Cybern 71: 401–416

Srinivasan MV (1998) Insects as Gibsonian animals. Ecol Psycol 10: 251–270

Srinivasan MV, Zhang SW, Lehrer M, Collett TS (1996) Honeybee navigation en route to the goal: visual flight control and odometry. J Exp Biol 199: 237–244

Wagner H (1982) Flow-field variable trigger landing flies. Nature 297: 147–148

Zeil J (1993) Orientation flights of solitary wasps (Cerceris; Sphecidae; Hymenoptera). I. Description of flight. J Comp Physiol [A] 172: 189–205